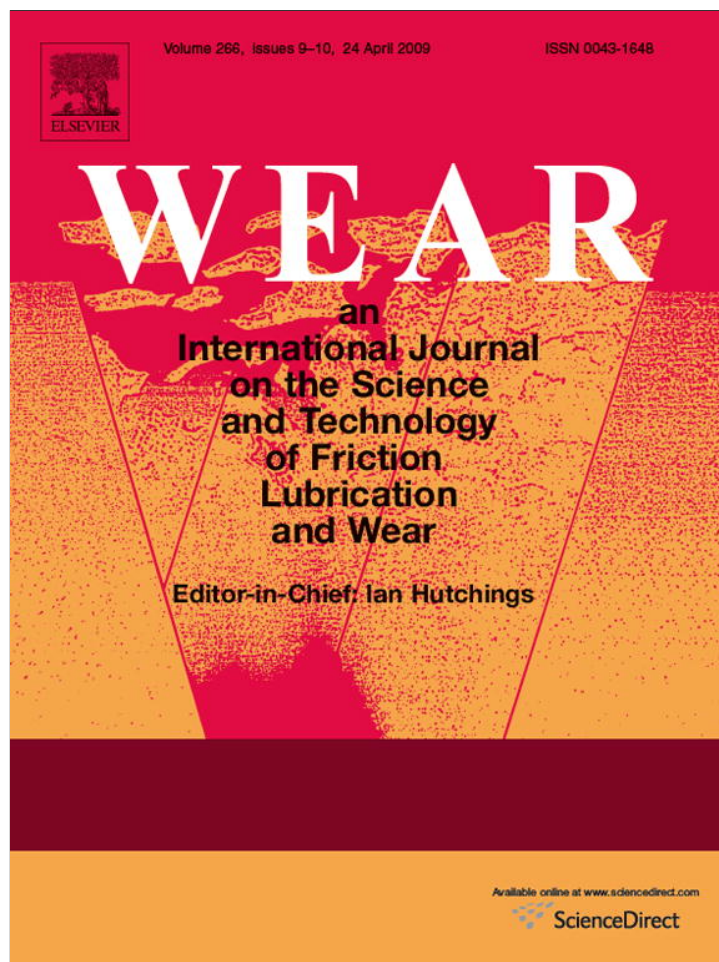


Provided for non-commercial research and education use.
Not for reproduction, distribution or commercial use.



This article appeared in a journal published by Elsevier. The attached copy is furnished to the author for internal non-commercial research and education use, including for instruction at the authors institution and sharing with colleagues.

Other uses, including reproduction and distribution, or selling or licensing copies, or posting to personal, institutional or third party websites are prohibited.

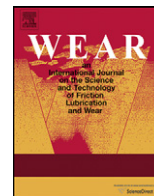
In most cases authors are permitted to post their version of the article (e.g. in Word or Tex form) to their personal website or institutional repository. Authors requiring further information regarding Elsevier's archiving and manuscript policies are encouraged to visit:

<http://www.elsevier.com/copyright>



Contents lists available at ScienceDirect

Wear

journal homepage: www.elsevier.com/locate/wear

Third body effects in the wear of polyamide: Micro-mechanisms and wear particles analysis

A. Marcellan^{a,b}, O. Bondil^{a,b}, C. Boué^c, A. Chateauminois^{a,*}

^a Laboratoire de Physico-Chimie des Polymères et des Milieux Dispersés (PPMD), Ecole Supérieure de Physique et Chimie Industrielles (ESPCI), CNRS UMR 7615, Université Pierre et Marie Curie Paris VI (UPMC), 10, rue Vauquelin, 75231 Paris Cedex, France

^b Dutch Polymer Institute (DPI), Technische Universiteit Eindhoven, PO BOX 902, 5600 AX Eindhoven, The Netherlands

^c Laboratoire Photons et Matière (LPEM), Ecole Supérieure de Physique et Chimie Industrielles (ESPCI), CNRS UPR 5, Université Pierre et Marie Curie Paris VI (UPMC), 10, rue Vauquelin, 75231 Paris Cedex, France

ARTICLE INFO

Article history:

Received 28 May 2008

Received in revised form 4 December 2008

Accepted 10 February 2009

Available online 21 February 2009

Keywords:

Polyamide

PA 46

Wear

Third body

Molecular weight

Chain scission

ABSTRACT

The wear micro-mechanisms at a frictional interface between a polyamide 4,6 (PA 46) substrate and a spherical sapphire counterface have been investigated using *in situ* contact observation. Experiments were carried out under reciprocating sliding conditions with varying values of the overlap ratio, Δ , defined as the ratio of the displacement amplitude to the contact diameter. Using this procedure, it was found possible to vary the extent of wear particles accumulation within coherent third body agglomerates. For low overlap ratios ($\Delta < 0.2$), particles detached from the PA 46 substrate were extensively agglomerated within distinct third body corrugations. In this regime, the rate limiting process regarding the wear degradation was found to be the extrusion of fibril-like wear particles from the extremities of sheared third body agglomerates. On the other hand, no substantial debris accumulation was found to occur when the overlap ratio was greater than 0.2. Additional infrared thermal contact imaging showed that these wear mechanisms were induced under essentially isothermal conditions. From differential scanning calorimetry (DSC) and size exclusion chromatography (SEC) analysis, micro-structural changes within wear particles were found to be associated with a strong reduction in the molecular weight of the PA 46 molecules by virtue of stress-induced chain scission mechanisms.

© 2009 Elsevier B.V. All rights reserved.

1. Introduction

Polymers in their bulk and film forms are widely used as self-lubricating materials in many tribological applications where their wear resistance is of primary importance. In order to derive relevant wear models, much attention has been paid to the analysis of tribological damage micro-mechanisms in relation to surface mechanical properties (for a review, see for example Refs. [1–3]). Most of these analyses concentrate on the primary processes involved in the detachment of particles from the polymer surface. Within this context, scratching experiments have especially emerged over the past years, as a useful route to mimic and characterize the deformation and failure modes which occur as a consequence of specific interactions between asperities touching each other in discrete areas of contact between polymeric substrates and rough rigid counterfaces [4]. Such approaches provided insights into the elementary particles detachment mechanisms involved in the so-called abrasive wear situations [4,5]. However, particles detachment processes are only one of the facets of the

overall wear degradation. Investigations of interface tribology [6] have widely demonstrated that debris are usually trapped within the contact for varying periods of time during which they are subjected to a variety of mechanical and tribo-chemical processes and ultimately form what is often termed the ‘third body’. This third body plays an essential role in the way differences in the velocities between rubbing surfaces (the so-called ‘first bodies’) can be accommodated [7]. In the case of polymer surfaces, it often acts as a solid lubricant which reduces the stresses transmitted to the first bodies and ultimately decreases the wear rate. In a set of experiments where the level of third body accumulation within the contact was varied by changing the contact zone kinematics, Briscoe et al. [8,9] have shown that the wear rate of poly(methylmethacrylate) is primarily governed by the flow of distinct third body agglomerates under the action of shearing stresses. In such situations, the mechanical and rheological properties of third body compacts emerge as important parameters regarding the wear resistance of polymer systems. However, these properties are likely to be very different from that of the original substrate, as third body agglomerates are subjected to a variety of friction-induced mechano-chemical and/or mechano-physical changes. These processes have been especially investigated within the context of transfer film formation, which is a generic wear mechanism of

* Corresponding author. Tel.: +33 1 40 79 47 87; fax: +33 1 40 79 46 86.
E-mail address: antoine.chateauminois@espci.fr (A. Chateauminois).

many semi-crystalline polymers [10,11]. Complex tribo-chemical effects are known to occur during the formation of polymer transfer films to metal counterfaces, which are related to the molecular structure of the polymer, mating metal, friction and environmental conditions as well as to the presence of fillers.

The nature of the molecular mechanisms involved in transfer film and wear debris formation remains largely unsolved, as well as their relationships with the molecular and micro-structural characteristics of the virgin substrate. Using X-ray photoelectron spectroscopy (XPS) and Fourier transform Raman (FT-Raman) spectroscopy, Li et al. [12] have found evidence of the occurrence of both chain scission and oxidation during the sliding friction of poly(etheretherketone) (PEEK) against steel counterfaces. Similar conclusions were drawn from wear studies using polyamides materials, which are the subject of the present investigation. Using Fourier transform infrared microspectroscopy (FTIRM), Weick et al. [13] evidenced dissociation of the N–C bonds in the backbone of nylon 6,6 rubbed against sapphire. Size exclusion chromatography (SEC) analysis of the wear debris produced from PA 66/PA 66 contacts under mixed rolling/sliding conditions also showed a twofold reduction in the molecular weight as compared to the virgin polyamide substrate [14]. In a recent study, Cong et al. [15] concluded from infrared and X-ray spectroscopy that the strength of hydrogen bonds decreased in PA 46 transfer films and wear debris. It was also found by these authors that the amount of amorphous phase was increased in the transfer film and wear debris as compared to the virgin semi-crystalline substrate. For nylon 10,10 Wang et al. [16] showed that some hydrolysis of amide groups may occur in presence of water. The resulting decrease in hydrogen bonds between nylon 10,10 molecules was pointed out as an important factor that led to a high wear rate of nylon in water. The dependence of transfer film and wear debris formation on the molecular and micro-structural characteristics of polyamide substrates remains unclear. Samyn et al. [17,18] have observed that the nature of the catalyst used to polymerise polyamides can affect the softening of the material and the subsequent formation of a coherent transfer film during friction. The differences in softening mechanisms were correlated to structural changes evidenced by thermal analysis and Raman spectroscopy. In the case of oriented PA 6 fibres, Cayer-Barrioz et al. [19,20] also showed that the abrasive wear resistance was correlated to the level of molecular orientation within the amorphous phase, the later being varied when the molecular weight of the polyamide polymer was changed.

Changes in the crystallinity or in the molecular weight of wear particles can have a significant effect on third body rheology, which in turn can affect the ultimate wear properties of polymer systems. However, it is not clear whether these changes in the molecular and micro-structural characteristics of the wear debris only result from friction-induced increases in the contact temperature or if they can also occur under the purely mechanical action of the shearing stresses. In many of the above-mentioned studies, tribological conditions indeed resulted in a substantial heating – and even melting – of the polymer surfaces.

Within the framework of this study, third body formation and flow within a PA 46/sapphire contact were investigated under essentially isothermal contact conditions. By changing the relative displacement amplitude under reciprocating sliding conditions, it was found possible to vary the extent of wear particles accumulation and compaction within third body agglomerates. The associated wear micro-mechanisms were investigated from in situ contact observation through the transparent counterface. Infrared contact imaging also allowed evaluating the temperature rise at the worn contact interface. In addition, some of the features of wear processes, such as the extrusion of fibril-like debris from third body corrugations, were qualitatively accounted for from SEC and differ-

ential scanning calorimetry (DSC) analysis of the microstructure and molecular weight distribution of the wear particles.

2. Materials and experimental details

2.1. Polyamide material

The selected PA 46 was a commercial Stanyl TW200 grade provided by DSM (Geleen, Netherlands). This polymer was processed from dried pellets in the form of injection moulded bars 4 mm in thickness and 10 mm in width. The bars were cut into parallelepiped specimens (10 mm × 10 mm × 4 mm) for the wear tests. They were subsequently cleaned with ethanol and hexane and rinsed with distilled water. Prior to wear testing, the samples were dried 12 h under vacuum at 80 °C and stored in a desiccator. The sliding direction was set perpendicular to the injection flow direction.

2.2. Wear experiments

Wear experiments were carried out using a home-made reciprocating tribometer fully described in Refs. [21,22]. The flat PA 46 specimens were rubbed at imposed displacement amplitude against a smooth ($R_a < 5$ nm) plano-convex sapphire lens (Melles Griot, France) with a radius of curvature of 7.7 mm. Unless otherwise specified, all the experiments were carried out at a constant applied normal load of 200 N. The corresponding initial mean contact pressure was close to 110 MPa and yielded a contact radius of about 750 μm . The wear experiments were repeated at various imposed relative displacements between 0.3 and 2 mm, while the sliding velocity was kept constant and equal to 2 mm s⁻¹. The number of sliding cycles was varied between 2.5×10^3 and 10^5 cycles. Optical microscopy observations did not reveal any substantial wear damage of the sapphire lens. During the experiments, the relative displacement and the tangential force were continuously monitored. Polyamide materials being very sensitive to water plasticization, special care was taken in order to ensure controlled environmental conditions during the tests. For that purpose, an environmental cell was designed which allowed performing the wear tests under a dry air flow. Prior to injection within the cell, compressed air was dried out within columns filled with silica gel. This procedure provided a relative humidity less than 10% around the specimens during the course of the wear tests.

An optical zoom equipped with a CCD camera also allowed in situ video recording of images of the contact area through the sapphire lens. Alternatively, in situ infrared thermal contact imaging was performed using a CEDIP JADE MWIR InSb camera with 320×256 pixels (pixel size of 30 $\mu\text{m} \times 30 \mu\text{m}$) and a 3–5.1 μm wavelength band detection. The thermal sensitivity of the system is 20 mK. It was calibrated prior to the experiments using a black body. While the polymer underwent cyclic sliding, the IR camera was coupled with a “lock-in” device and the system processor accumulated dated infrared images at the frame frequency (100 Hz). Mathematical signal processing (FFT, filters) allowed to compute the amplitude and the phase of the infrared distribution at the frequency of the modulated contact loading. The contact temperature was calculated from the IR signal assuming that the sapphire counterface was transparent to infrared and that the emissivity of the PA 46 surface was close to 1.

2.3. Differential scanning calorimetry

The melting and crystallization behaviour of the PA 46 wear particles was investigated using differential scanning calorimetry (DSC 2920, TA instruments). All experiments were carried out under dry nitrogen flow using aluminium pans. Two successive melting/crystallization cycles were applied to the material. The

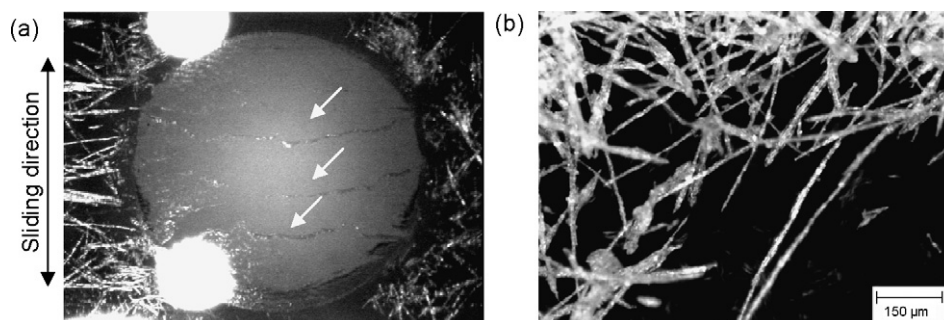


Fig. 1. Wear damage mechanisms of the PA 46 substrate under a low overlap ratio condition ($\Delta=0.13$, 2×10^4 cycles). (a) In situ observation of the wear scar showing the formation of third body corrugations (as indicated by the white arrows) oriented perpendicularly to the sliding direction. (b) Details of the fibril-like wear debris displaced from the extremities of the third body corrugations.

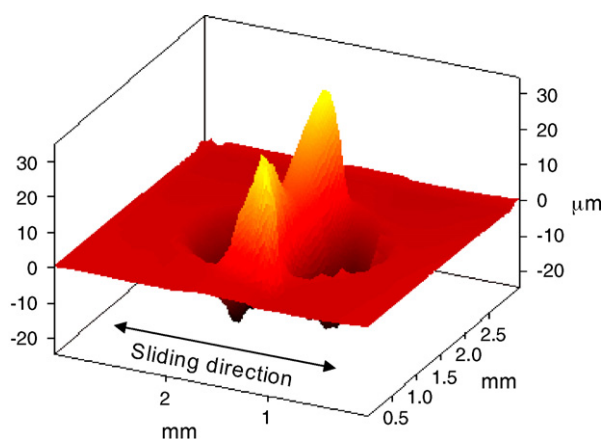


Fig. 2. Topography of a wear scar produced under a low overlap ratio condition ($\Delta=0.19$, 2×10^4 cycles).

specimens (about 10 mg) were submitted to a first temperature scan at 5 C/min from 30 up to 310 C. After a 10 min isothermal step at 310 C, the polymer was cooled down to 30 C at 5 C/min and subsequently re-heated at 5 C/min up to 310 C. In some complementary experiments, an additional isothermal step (30 min at 240 C) was applied to the specimen prior to the first melting step in order to stabilize the crystalline microstructure.

2.4. Size exclusion chromatography

The molecular weight distribution of PA 46 wear particles was determined by means of size exclusion chromatography using an Hewlett Packard 1090M2 apparatus equipped with refractive index (RI), UV (270 nm) and differential viscosimeter detectors. Virgin PA

46 and wear particles specimens were dissolved in hexafluoroisopropanol with 0.1 wt% potassium trifluoro acetate for more than 4 h. In all cases, some undissolved particles were still visible. The samples were filtered ($0.45 \mu\text{m}$) before injection within the SEC column, so only soluble part of the sample was analysed. The concentration of this soluble part was estimated using the RI data for a linear reference PA 46 normalized with respect to the injected mass. It was assumed that the wear particles samples have the same dn/dc (refractive index increment) than that of the reference PA 46. Using this assumption, it was found that about 95% of each sample had dissolved. The molecular weight distributions were obtained using an universal calibration procedure. The average errors on the different molecular mass distribution moments (M_n , M_w) are $\pm 10\%$.

3. Wear micro-mechanisms

3.1. In situ observations

Wear micro-mechanisms were investigated from a set of cyclic sliding experiments carried out at increasing values of the overlap ratio, Δ , which was defined as the ratio of the applied displacement amplitude to the initial value of the contact diameter. This procedure was used in order to vary the extent of wear particles trapping at the contact interface. Indeed, in situ contact observations through the transparent sapphire counterfaces revealed the occurrence of two different kinds of wear damage mechanisms depending on the value of the overlap ratio.

For the lowest overlap ratios ($\Delta < 0.2$), wear damage was associated with the development of distinct third body agglomerates in the form of thin corrugations which were regularly spaced and oriented perpendicularly to the sliding direction (Fig. 1a). In situ observations showed that these third body agglomerates were extensively sheared during the sliding cycle, but that they were not

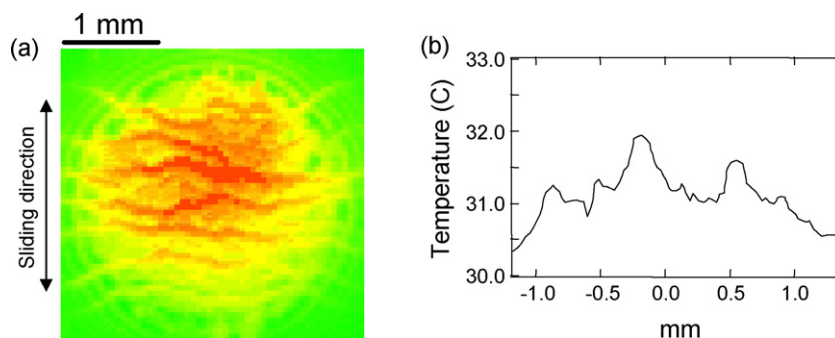


Fig. 3. In situ infrared imaging of the contact during the early stages of the wear process under a low overlap ratio condition ($\Delta=0.13$, 5×10^3 cycles). (a) distribution of the amplitude of the infrared signal within the contact zone showing the localization of frictional energy dissipation within third body corrugations. (b) Temperature profile along the sliding direction.

rolling as it can be the case for rubber-like materials which form similar third body agglomerate during large amplitude frictional sliding [23]. Once these third body formations were stabilized at the contact interface, fibril-like wear debris about 10–30 μm in diameter (Fig. 1b) were displaced from the extremities of the third body corrugations according to a mechanism which is reminiscent of the extrusion of a melt or a paste. During the course of the tests, these corrugations eventually merged into a single ripple (Fig. 2). Similar third body formations were already observed under reciprocating contacts between poly(methylmethacrylate) (PMMA) and steel counterface [8,9], where they were explained from a consideration of the changes in the contact zone kinematics which result from the load-carrying capacity of the wear debris agglomerates. Early fretting investigations also mentioned similar wear mechanisms for PA 66 and polycarbonate [24,25]. All these observations tend to indicate that fibril-like debris formation from third body agglomerate can be considered as a generic feature of polymer contacts under low amplitude sliding micro-motions.

The formation of coherent third body agglomerates and their extrusion in the form of fibrils raises the question of the temperature at the frictional contact interface. In order to address this issue, infrared contact imaging was carried out through the sapphire counterface. Fig. 3 shows an example of the measured contact temperature distribution for an overlap ratio, $\Delta = 0.19$. The figure clearly shows the occurrence of a localized temperature rise within the third body ripples. It turns out that third body generates a load-carrying capacity within the contact which tends to separate the rubbing substrates. As a result, a large part of the frictional energy is dissipated within the third body agglomerate. As shown by the temperature profile in Fig. 3, the corresponding temperature increase remains, however, limited to a few degrees. The high thermal conductivity of the sapphire lens (about 80 times higher than that of the PA 46 substrate) can at least partly account for this limited temperature increase. As a conclusion, IR measurements show that, for the tribological conditions under investigation, no surface melting effects are involved in the generation and flow of the third body.

When the overlap ratio was increased above about 0.2, in situ observations showed the disappearance of the third body corrugations. Most of the wear debris then appeared to be expelled from the extremities of the wear tracks in the form of flakes, without evidence of substantial fibrils formation as it was the case under small amplitude micro-motions (Fig. 4). An examination of the tangential force/displacement loops provides some insight into the associated mechanisms (Fig. 5). As extensive wear damage proceeded under more and more conformal contact conditions, an increase in the tangential force was observed at the end of the forward and backward sliding motions, just before the sliding direction was reversed. This increase can be attributed to the ploughing of the ends of the ellipsoidal wear tracks by the rigid spherical counterface. Accordingly, the formation of flake-like debris within this region is due to the repeated shearing of the PA surface by the sapphire counterface at the extremities of the wear track.

To summarize, two different wear damage mechanisms were identified as a function of the overlap ratio. For low overlap ratios, a third body regime was identified where the rate limiting process for wear degradation is the displacement of fibril-like debris from the extremities of stable wear particles agglomerates which are trapped within the contact interface. On the other hand, large overlap ratios were associated with an essentially 'two bodies' wear regime with no significant third body accumulation within the contact. As shown in Fig. 6, these changes in the wear micro-mechanisms were not correlated with any very significant difference in the level of friction. Only a slight increase in the coefficient of friction was observed when the overlap ratio was increased from 0.2 to 1.35 (i.e. the sliding amplitude was increased from about 0.3 to 2 mm).

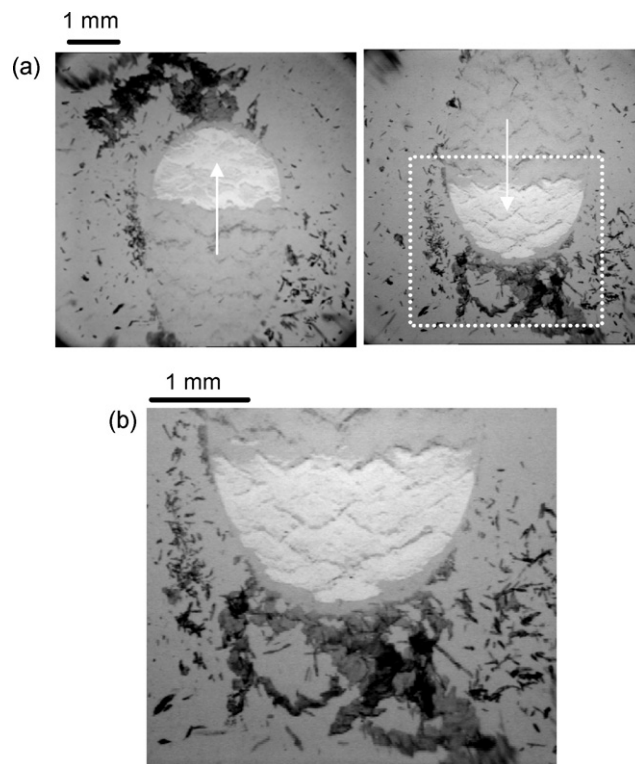


Fig. 4. Wear damage mechanisms of the PA 46 substrate under a high overlap ratio condition ($\Delta = 1.35$, 5×10^4 cycles). (a) In situ observations of the contact area corresponding to the two extremes positions of the sapphire lens during the sliding cycle (sliding direction indicated by the white arrow). No distinct third body corrugation is observed and flake like wear debris are essentially displaced from the extremities of the contact. (b) Detail corresponding to the white dotted area in (a) showing the formation of flake like wear debris.

3.2. Wear volumes

From a more quantitative point of view, a volumetric wear analysis was carried out from a topographical analysis of the wear scars at the end of the wear experiments. These measurements were performed at different overlap ratios and for increasing number of cycles. In order to account for the changes in the sliding amplitude and in the number of cycles, the wear volumes were reported

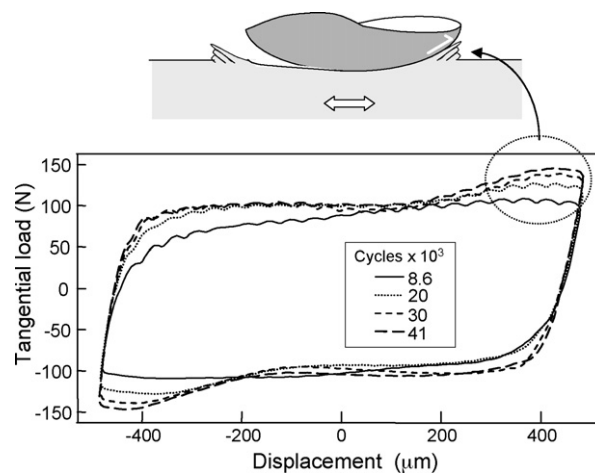


Fig. 5. Tangential force/displacement loops recorded as a function of the number of cycles for an overlap ratio, $\Delta = 0.6$. As shown in the schematic picture, the final increase in the tangential load on the friction plateau is due to the ploughing of the extremities of the semi-ellipsoidal wear tracks by the rigid spherical counterface. Wear particles are produced by the shearing action of the rigid spherical slider.

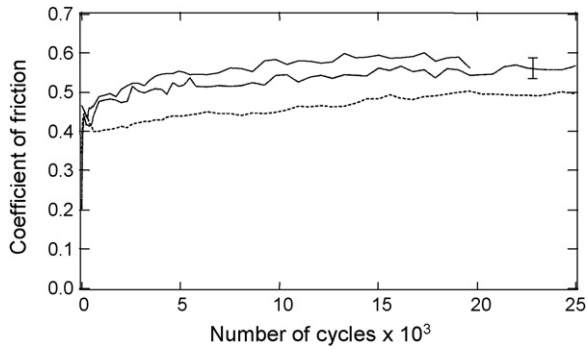


Fig. 6. Coefficient of friction as a function of the number of sliding cycles for different overlap ratios (small dotted lines: $\Delta = 0.19$, large dotted line: $\Delta = 0.66$, continuous line: $\Delta = 1.35$).

in Fig. 7 as a function of the cumulated frictional energy dissipated during the wear experiments. These energies were obtained from an integration of the load/displacement loops which were continuously monitored during the tests.

It emerges from Fig. 7 that the resistance of the PA 46 substrate to frictional energy dissipation is strongly increasing when the overlap ratio is reduced. These differences can be related to the observed changes in the wear micro-mechanisms. As indicated by the wear scars profiles reported in Fig. 8a, the wear experiments with $\Delta = 0.19$ were associated with a ‘third body regime’ characterized by the accumulation and compaction of the wear particles within a central corrugation. On the other hand, overlap ratios of 0.66 and 1.35 correspond to an essentially two body regime with limited wear debris accumulation within the contact zone. For $\Delta = 0.19$, it was also observed that the central third body ripple progressively disappeared as the number of cycles was increased above about 10^4 cycles (Fig. 8b), i.e. when the total frictional dissipated energy exceeded about 500J. In Fig. 7, it can be seen that above this threshold, the sensitivity of PA 46 to frictional energy dissipation is enhanced, as indicated by the increased slope of the wear volume/dissipated energy relationship. This observation further emphasises the correlation between the presence of third body corrugations and the resistance of the PA 46 substrate to wear damage.

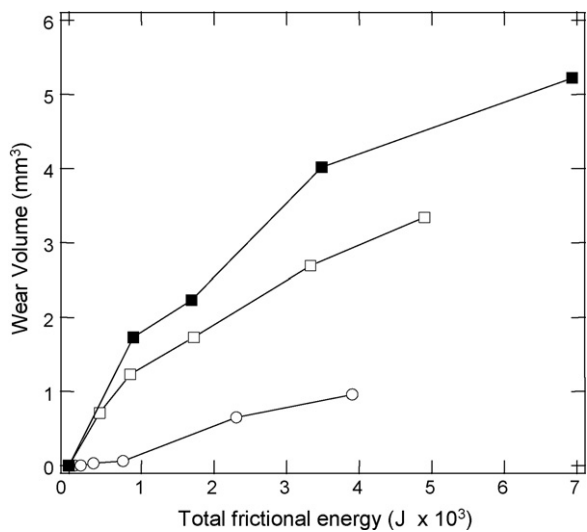


Fig. 7. Wear volumes as a function of the cumulated frictional energy dissipated within the contact. (○) $\Delta = 0.19$; (□) $\Delta = 0.66$; (■) $\Delta = 1.35$. For each of the considered overlap ratios, the total frictional energy was varied by changing the number of sliding cycles.

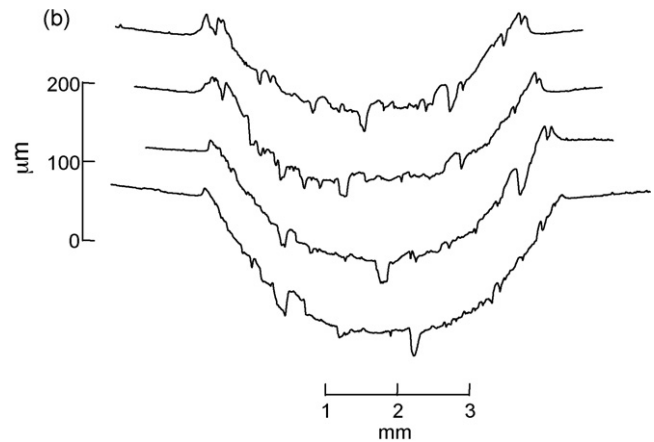
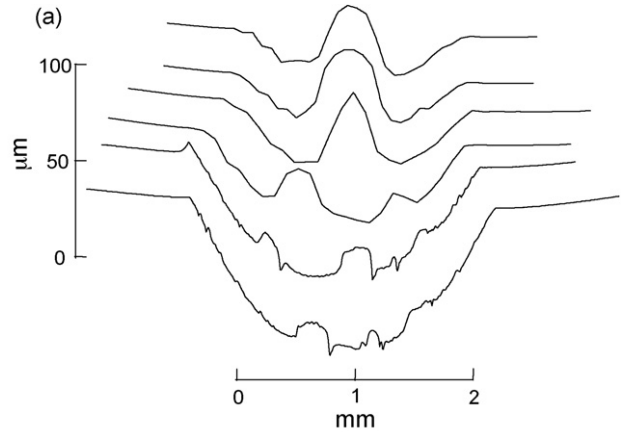


Fig. 8. Wear scars profiles after increasing number of sliding cycles. (a) Overlap ratio, $\Delta = 0.19$. From top to bottom: 2.5, 5, 10, 20, 63 and 100×10^3 cycles. (b) Overlap ratio, $\Delta = 1.35$. From top to bottom: 2.5, 5, 10 and 20×10^3 cycles. The profiles were taken in the middle of the wear scars and perpendicular to the sliding direction.

As a conclusion, it turns out that wear particles compaction within stable third body agglomerates has a beneficial effect on the wear resistance of polyamide substrates. In other words, the trapped third body at the contact interface acts as a solid lubricant which prevents additional wear particles from being detached from the substrate. Such a “third body” situation is favoured under low amplitude micro-motions due to high overlap of the contact zone. Under such conditions, it appears that the wear rate is primarily dependent on the extrusion of fibrils from distinct third body agglomerates, under the combined action of normal and shear stresses. In the absence of any substantial heating of the contact, this mechanism suggests that the agglomerated wear debris could have significantly reduced mechanical properties as compared to the virgin, semi-crystalline, PA 46 substrate. Such differences could result from the fact that the micro-structural and molecular properties of the agglomerated wear debris differ largely from that of the semi-crystalline substrate which they originate from. In order to elucidate this point, DSC and SEC characterizations were carried out on wear particles.

4. Wear particles analysis

4.1. Melting and crystallization behaviour

As a baseline, the melting behaviour of the virgin PA 46 specimen was first investigated. In order to detect any potential micro-structural gradient resulting from the injection moulding process,

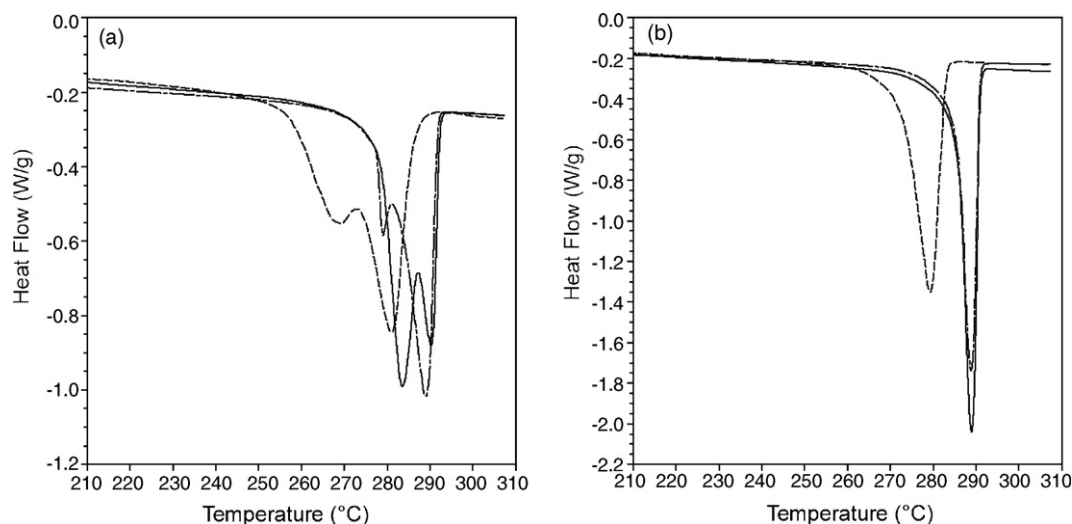


Fig. 9. Melting behaviour of the virgin PA 46 substrate and of the wear particles, as determined by differential scanning calorimetry (DSC, 5 °C/min). (a) First temperature scan and (b) second temperature scan. Solid line: core of the virgin PA 46 specimen; broken dash: surface of the virgin PA 46 specimen; short dash: wear particles.

specimens were taken from both the core and the surface of the PA 46 bars. During the first temperature scan, the melting peak shows a well-defined splitting (Fig. 9): two different crystallite populations are identified. Such a splitting of the melting peak has already been reported for PA 46/PA 6 yarns by Schmack et al. [26]. These authors attributed the first melting peak to relatively unstable crystallites, which are reorganized during the temperature scan and subsequently melt at the temperature of the second melting peak. During the second temperature scan, the melting behaviour appears to be strongly modified: only a very sharp melting peak is noted at about 289 °C, with no evidence of splitting. The first melting/crystallization cycle has therefore largely modified the initial microstructure of the specimen. The thermograms in Fig. 9 also show a difference between the melting behaviour of the surface and the core of the virgin PA 46 specimens. It can be attributed to the micro-structural gradients which result from the thermal and mechanical gradients encountered during injection moulding. However, a detailed analysis of these effects is out of the scope of this wear study.

The experiments were repeated using the wear debris generated under large overlap ratio conditions, i.e. $\Delta = 1.35$ (for lower overlap ratios, the amount of wear particles was too small to allow for a DSC analysis). As compared to the virgin substrate, the most important change is a depression of the melting temperature T_m (Table 1). This decrease in T_m was still observed during a second temperature scan, which shows that it results from a permanent change in the PA 46 structure. This decrease in the melting temperature can be attributed to two different effects. The first one is a decrease in the crystal size or in the crystalline perfection within the wear debris specimens as a result of the mechanical action of

the shearing stresses which are experienced by the polymer during the formation of the wear particles. The second explanation for the observed depression in the melting temperature is a potential decrease in the molar mass of the polymer. Indeed, the influence of the molecular weight on T_m has already been extensively reported in the literature [27–29]. The fact that T_m is still depressed during the second heating scan tends to rather support this hypothesis of a decrease in the molecular weight, as the effects of a change in the crystallite size/perfection would probably be – at least partly – suppressed after the first melting/crystallization cycle.

An examination of the effects of an isothermal step at 240 °C prior to melting is also interesting (Table 1). For the virgin PA 46 surface, it resulted in a limited change in the melting temperatures and enthalpies. In the case of the wear particles, it can be noted that the isothermal step below T_m results in increased melting temperature and enthalpy. This could be interpreted as an evidence of an enhanced reorganization/recrystallization of the wear particles during the isothermal step (the original properties of the PA 46 substrate were, however, not recovered). Such an interpretation is consistent with the hypothesis of a reduction in the molar mass of the polyamide within the wear debris, which in turn enhances the mobility of the polymer chains and the ability for the crystallites to reorganise.

As a conclusion, it comes out that the molecular and micro-structural characteristics of the wear particles generated during reciprocating sliding are largely different from that of the virgin PA 46 substrate. The DSC analysis tends to demonstrate that the molecular weight of the PA 46 material is reduced during the wear process. This hypothesis was further confirmed by the SEC experiments described below.

Table 1

Melting behaviour of the virgin PA 46 and the wear particles generated after 10^4 cycles (overlap ratio $\Delta = 1.35$).

	Virgin PA 46 surface	Wear particles
Temperature scan from R.T.		
T_m (°C)	293.4 (0.5)	283.3
ΔH_m (J/g)	83.6 (2.7)	52.3
Temperature scan after isothermal step at 240 °C		
T_m (°C)	292.4 (0.4)	287.2
ΔH_m (J/g)	72.2 (3.5)	90.6

T_m and ΔH_m refer to the melting temperature and enthalpy, respectively (standard deviations within brackets).

4.2. Molecular weight distribution

The SEC analysis revealed a very important decrease (by a factor of about 7) in both the weight (M_w) and number (M_n) average molecular weights of the PA 46 polymer within the wear debris, which indicates the occurrence of intensive chain scission during the course of the wear process (Table 2). As mentioned in the introduction, a twofold reduction in M_n and M_w was reported by Apichartpattanasri et al. [14] from the SEC characterization of the wear particles produced from a polyamide 6,6 substrate. However, this study was performed using a twin-disk machine operated under contact conditions where a significant melting of

Table 2

Molecular mass distribution of the virgin PA 46 and the wear particles as measured by size exclusion chromatography (SEC).

Sample	M_n (kg/mole)	M_w (kg/mole)	M_w/M_n
Virgin PA 46	23	65	2.82
PA 46 wear particles	3.2	9.8	2.73

Wear particles were generated using an overlap ratio, $\Delta = 1.35$, and 10^4 sliding cycles.

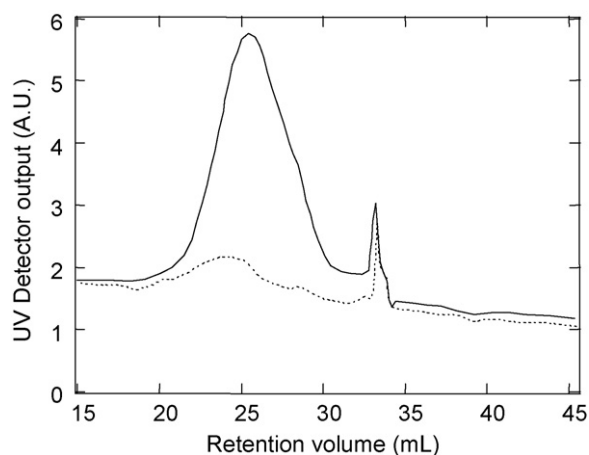


Fig. 10. Output of the UV detector used during size exclusion chromatography (SEC, 270 nm). Solid line: wear particles; dotted line: virgin PA 46 substrate.

the polymer surface occurred. The difference here is that molecular weight reduction takes place without any substantial temperature increase at the contact interface. It therefore turns out that, in the present situation, chain scission is essentially a mechano-chemical effect induced by the repeated action of the shear stress within the third body agglomerates.

In addition, the output of the UV detector of the SEC showed a considerable amount of absorption of the wear particles specimens, while virgin PA 46 does not show much UV absorption at the considered wavelength (270 nm) (Fig. 10). There is therefore some evidence that the wear particles have a chemical composition which differs from that of virgin Stanyl. Some oxidation could be envisaged during the course of the wear tests. As suggested by Weick et al. [13] in the case of PA 66 rubbing against sapphire, chain scission in polyamide materials are likely to involve the breakage of the N–C bonds which results in the formation of UV absorbing species which are enriched in carbonyl groups.

Stress-induced chain scission mechanisms in bulk polymers are a well documented topic which has been extensively reviewed in a book by Kausch [30]. During dynamic straining of polymers, very large axial forces can be transferred onto extended chain segments. These forces are sufficient to cause the scission of a chain molecule into organic radicals. Once formed, the highly reactive chain end radicals can react with oxygen to form chemical groups such as aldehyde, esters, carbonyl or carboxyl groups. Such chemical processes could account for the enhanced UV adsorption of the PA 46 wear debris molecules. Interestingly, oriented polymers with little potential of plastic deformation such as polyamide fibres were found to be particularly suitable systems for the investigation of mechanical chain breakage mechanisms, in view of the fact that the slippage of the chains reduces or prevents mechanical scission. In the investigated wear situation, it is therefore possible that chain scission is enhanced by virtue of friction-induced molecular orientation of the surface layers. It has also been reported that chain scission is activated at high strain rates [30], while very high strain rates can be achieved within the polymer layers confined close to a sliding interface. Friction therefore emerges as a particularly suit-

able situation for the activation of chain scission mechanisms in polymer systems.

5. Conclusion

The contribution of third body formation to the wear degradation of a PA 46 substrate rubbing against a sapphire counterface has been investigated under reciprocating sliding conditions. When the sliding amplitude was less than the contact diameter, wear particles detached from the polyamide substrate were found to be preferentially accumulated and compacted within distinct third body corrugations. Under such conditions, the rate limiting process regarding wear degradation was the flow of fibril-like wear particles from the third body agglomerates. This 'three bodies' wear situation was characterized by a reduced sensitivity to frictional energy dissipation as compared to the predominantly 'two bodies' wear situations encountered under large amplitude sliding motions. Physical-chemistry investigations of the wear particles show that wear particle generation and migration within the contact interface is associated with strong changes in the polymer microstructure and molecular characteristics, even under tribological conditions where no substantial increase in contact temperature is involved. Of particular significance is the strong decrease in the molecular weight of the polyamide material as a result of stress-induced chain scission mechanisms. Such a decrease can account for the ability of third body to flow from the contact in the form of fibrils. These mechanisms were identified for a PA 46 substrate rubbing against a sapphire counterface. However, stress-induced chain scission mechanisms are likely to be relatively independent on the nature of the counterface, provided that a high enough level of friction is maintained within the contact interface. In that view, the identified molecular wear damage mechanisms are probably generic of many practical tribological situations involving polyamide materials, such as gears or bearings, where wear particle trapping is enhanced by either slip micro-motions or conformal contact conditions.

Acknowledgements

This study was carried out within the frame of the Research Programme of the Dutch Polymer Institute (DPI), Eindhoven, The Netherlands, project #465. The authors also wish to thank Harold van Melick and Hans van Dijk (DSM, Geleen, Netherlands) for their support in the manufacturing of the specimens and in the SEC analysis. This work also benefited from stimulating discussions with Richard van den Hof (DSM, Geleen, Netherlands). Many thanks are also due to Damien Favier (ICS, Strasbourg) for the profilometry measurements.

References

- [1] B.J. Briscoe, *Wear of polymers: an essay on fundamental aspects*, *Tribology International* 14 (1981) 231–243.
- [2] B.J. Briscoe, S.K. Sinha, *Wear of polymers*, *Proceedings of the Institution of Mechanical Engineers Part J-Journal of Engineering Tribology* 216 (J6) (2002) 401–413.
- [3] J.K. Lancaster, *Friction and wear*, in: A.D. Jenkins (Ed.), *Polymer Science, A Material Science Handbook*, North-Holland Publishing Company, 1972, p. 959, Chap. 14.
- [4] B.J. Briscoe, *Isolated contact stress deformations of polymers: the basis for interpreting polymer tribology*, *Tribology International* 31 (1–3) (1998) 121–126.
- [5] A.C.M. Yang, T.W. Wu, *Wear and friction in glassy polymers: microscratch on blends of polystyrene and poly(2,6-dimethyl-1,4-phenylene oxide)*, *Journal of Polymer Science B: Polymer Physics* 35 (1997) 1295–1309.
- [6] M. Godet, *The third body approach: a mechanical view of wear*, *Wear* 100 (1984) 437.
- [7] Y. Berthier, M. Godet, M. Brendlé, *Velocity accommodation in friction*, *Tribology Transactions* 32 (4) (1989) 490–496.
- [8] B.J. Briscoe, et al., *Fretting wear behaviour of PMMA under linear motions and torsional contact conditions*, *Tribology International* 31 (11) (1998) 701–711.

- [9] B.J. Briscoe, et al., Contact damage of poly(methylmethacrylate) during complex micro-displacements, *Wear* 240 (2000) 27–39.
- [10] S. Bahadur, The development of transfer layers and their role in polymer tribology, *Wear* 245 (2000) 92–99.
- [11] G. Jintang, Tribochemical effects in formation of polymer transfer film, *Wear* 245 (2000) 100–106.
- [12] T.Q. Li, et al., Friction induced mechanochemical and mechanophysical changes in high performance semicrystalline polymer, *Polymer* 40 (1999) 4451–4458.
- [13] B.L. Weick, et al., Tribochemical changes of Nylon-6,6 and Nylon-6,6/Glass rubbed against sapphire, *Tribology Transactions* 37 (1) (1994) 129–137.
- [14] S. Apichartpattanasiri, J.N. Hay, S.N. Kukureka, A study of the tribological behaviour of polyamide 66 with varying injection-moulding parameters, *Wear* 250 (2001) 1557–1566.
- [15] P. Cong, et al., Morphology and microstructure of polyamide 46 wear debris and transfer film: a relation to wear mechanisms, *Wear* 265 (2008) 1100–1105.
- [16] J.X. Wang, M.Y. Gu, Wear properties and mechanisms of nylon and carbon-fiber-reinforced nylon in dry and wet conditions, *Journal of Applied Polymer Science* 93 (2) (2004) 789–795.
- [17] P. Samyn, et al., Friction, wear and transfer of pure and internally lubricated cast polyamides at various testing scales, *Wear* 262 (11/12) (2007) 1433–1449.
- [18] P. Samyn, et al., Softening and melting mechanisms of polyamides interfering with sliding stability under adhesive conditions, *Polymer* 47 (14) (2006) 5050–5065.
- [19] J. Cayer-Barrioz, et al., Abrasive wear micromechanisms of oriented polymers, *Polymer* 45 (8) (2004) 2729–2736.
- [20] J. Cayer-Barrioz, et al., On the correlation abrasive wear resistance—molecular weight: a quantitative wear law for polymeric fibres, *Wear* 261 (3/4) (2006) 460–466.
- [21] J.F. Lamethe, et al., Contact fatigue behaviour of glassy polymers with improved toughness under fretting wear conditions, *Wear* 255 (2003) 758–765.
- [22] E. Gacoin, A. Chateauminois, C. Fretigny, Measurements of the viscoelastic moduli of an acrylate polymer in bulk and film form using a contact method, *Polymer* 45 (2004) 3789–3796.
- [23] S.M. Aharoni, Wear of polymers by roll formation, *Wear* 25 (1973) 309–327.
- [24] F.H. Stott, B. Bethune, P.A. Higham, Fretting induced damage between contacting steel-polymer surfaces, *Tribology International* 10 (4) (1977) 211–215.
- [25] B. Bethune, The surface cracking of glassy polymers under a sliding spherical indenter, *Journal of Materials Science* 11 (1976) 199–205.
- [26] G. Schmack, R. Schreiber, Relation between molecular orientation and mechanical properties in differently processed polyamide 4,6/6 textile yarns, *Journal of Applied Polymer Science* 66 (2) (1997) 377–385.
- [27] D. Garcia, H.W. Starkweather, Hydrogen-bonding in Nylon-66 and model compounds, *Journal of Polymer Science Part B-Polymer Physics* 23 (3) (1985) 537–555.
- [28] H.W. Starkweather, P. Zoller, G.A. Jones, The heat of fusion of 66-Nylon, *Journal of Polymer Science B: Polymer Physics* 22 (9) (1984) 1615–1621.
- [29] P.J. Flory, Thermodynamics of crystallization in high polymers. 4. A theory of crystalline states and fusion in polymers, copolymers, and their mixtures with diluents, *Journal of Chemical Physics* 17 (3) (1949) 223–240.
- [30] H.H. Kausch, *Polymer fracture. Polymers. Properties and Applications*, vol. 2, Springer-Verlag, Berlin, 1978.